Andrzej RYNIEWICZ[1]

[1] University of Applied Sciences in Nowy Sącz, Faculty of Engineering Sciences, Zamenhofa 1a, 33-300 Nowy Sącz, e-mail: aryniewicz@ans-ns.edu.pl

Assessment of shape reproduction in computed tomography using reference spheres

Abstract

The aim of this study was to evaluate the accuracy of shape reproduction in computed tomography using reference spheres. Measurements were carried out with Siemens Somatom Sensation 64 and Werth Tomo Scope Compact scanners, with data analyzed in the Amira system. The workflow included segmentation, interpolation, surface smoothing, and tetrahedral mesh generation. Diameter measurements revealed the influence of imaging parameters and object positioning on accuracy. The results confirm the usefulness of computed tomography as a control and measurement tool in both medicine and industry, enabling non-invasive assessment of complex geometries and comparison with CAD models.

Keywords: computed tomography, shape reproduction, reference spheres, 3D metrology, geometric analysis.

Ocena odwzorowania kształtu w tomografii komputerowej z zastosowaniem kul wzorcowych

Streszczenie

Celem pracy była ocena dokładności odwzorowania kształtu w tomografii komputerowej z wykorzystaniem kul wzorcowych. Badania przeprowadzono na skanerach Siemens Somatom Sensation 64 oraz Werth Tomo Scope Compact, a dane analizowano w systemie Amira. Proces obejmował segmentację, interpolację, wygładzanie powierzchni i generowanie siatek tetrahedralnych. Pomiary średnic kul wykazały wpływ parametrów obrazowania i pozycjonowania obiektu na uzyskiwaną dokładność. Uzyskane wyniki potwierdzają przydatność tomografii komputerowej jako narzędzia kontrolno-pomiarowego w medycynie i przemyśle, umożliwiającego nieinwazyjną ocenę geometrii złożonych elementów i porównanie ich z modelami CAD.

Słowa kluczowe: tomografia komputerowa, odwzorowanie kształtu, kule wzorcowe, metrologia 3D, analiza geometryczna.

1. Introduction

A Computed tomography (CT) scanner is different from standard measuring devices in that, in addition to the external dimensions and shape of the object being examined, it allows for analysis of the object's internal structure (Ketcham, Mote, 2019). Tomographs can be used both in industry to assess the quality of examined objects – their geometry or internal structures – without destroying them, and in medicine to analyze internal organs (Liu et al., 2024).

The problem of assessing the accuracy of element mapping is extremely important and has fascinated scientists in various fields for years (Busch, Hausotte, 2024; Blažek et al., 2019). The latest spiral computed tomography (SCT) imaging techniques partially solve this problem, but determining 3D geometry still poses many challenges (Zemek et al., 2025). STC techniques do not allow for the simultaneous determination of the geometry of the structures of the objects under examination throughout the entire examination space with a certain degree of uncertainty (Bircher et al., 2021).

Ensuring that the shape of the examined surfaces is reproduced with sufficient accuracy (on a macro and micro scale) will allow for the assessment of the quality of parts in industry or medicine, the assessment of the condition of the examined organ, and a sufficiently rapid response to any changes that have occurred, which will contribute to the introduction of appropriate changes in the technological process or the making of an appropriate diagnosis (Stolfi, De Chiffre, Carmignato, 2016; Scherberich et al., 2025).

Figure 1. Ball patterns

(source: own study)

The first stage involved testing reference spheres (Figure 1) using Siemens Somatom Sensation 64 and Werth Messtechnik Tomo Scope Compact computed tomography scanners. The next step was to generate the surfaces of these elements in a 3D system and measure the dimensions of the spheres using Amira software.

Amira is a system used for 3D modeling and visualization. It allows for the visualization of scientific applications in various fields such as engineering, medicine, biology, chemistry, physics, and others. 3D objects can be represented as a mesh used for numerical simulations.

Using tomographs and analysis software, the diameters of the reference spheres were imaged and measured in two perpendicular planes (10 times each) for the following elements:

– reference sphere marked as Phantom 1 with a nominal diameter of Ø = 25.7 [mm];
– reference ball marked as Phantom 2 with a nominal diameter of Ø = 25.0 [mm];
– reference ball marked as Phantom 3 with a nominal diameter of Ø = 26.4 [mm].

2. Launch the Amira application

After launching the application, the main program window appears (Figure 2).

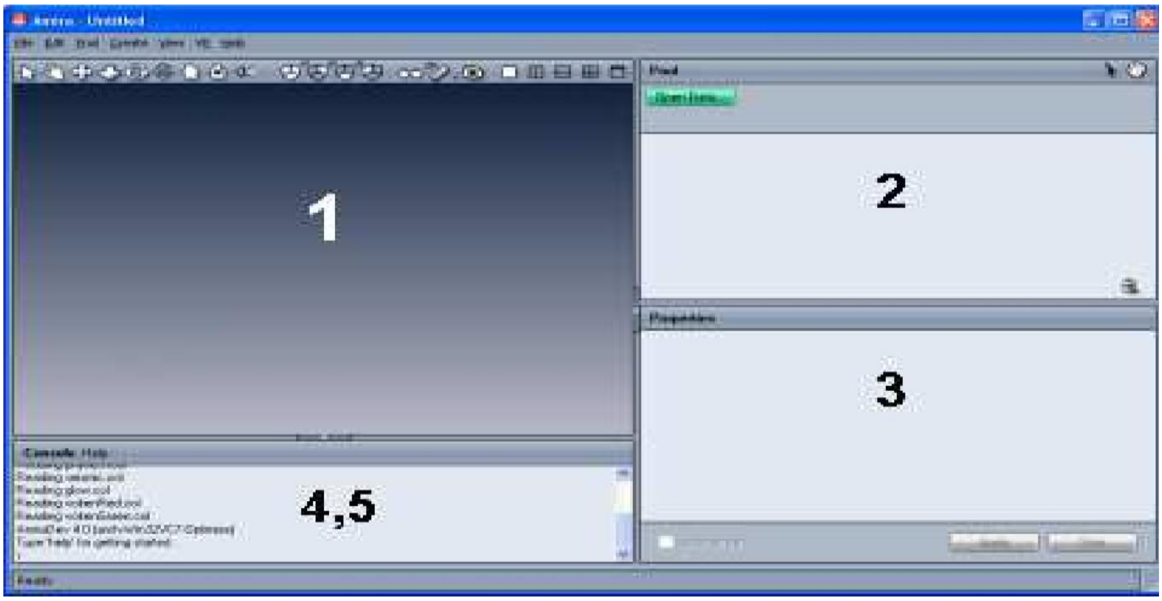

Figure 2. The application interface is divided into four-dimensional windows for visualization: (1) modular window, properties window (2), operations window (3), console window (4), and help window (5).

(source: own study)

3. Loading data received from computed tomography scanners

Data can be loaded in several ways (e.g., from File) and then on Open Data. After searching for the appropriate files obtained from tomographic diagnosis, they were loaded into the program.

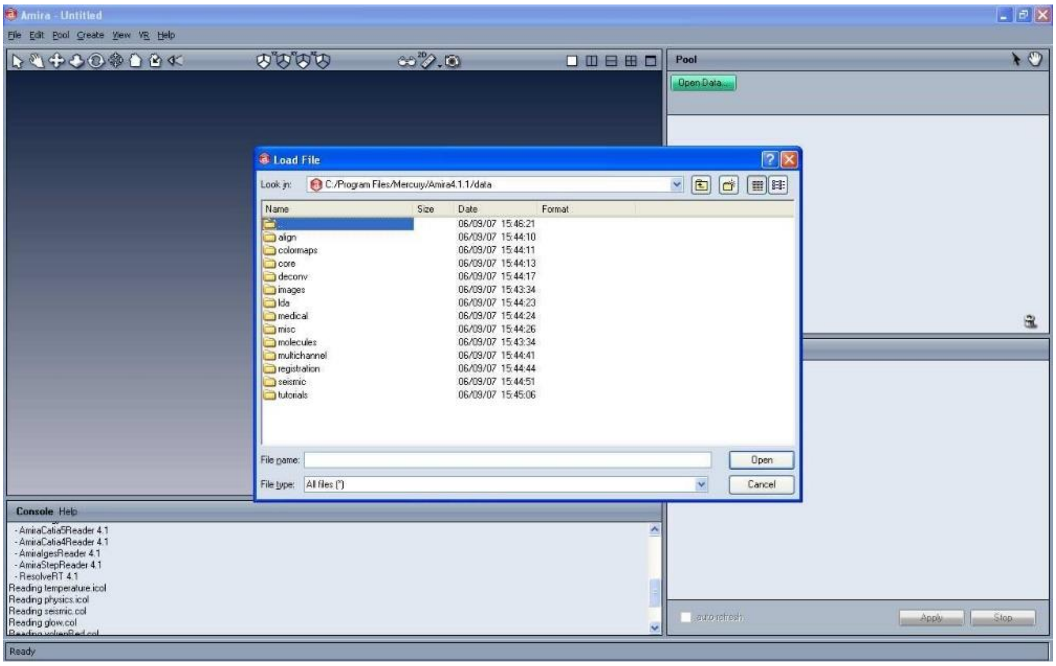

Figure 3. Loading data

(source: own study)

The loaded data appears in the module window as green icons with the .am extension (Figure 3). Each icon is a collection of related data from the tomograph. Clicking on an icon displays information in its properties window, such as the size or coordinates of the data (Figure 4).

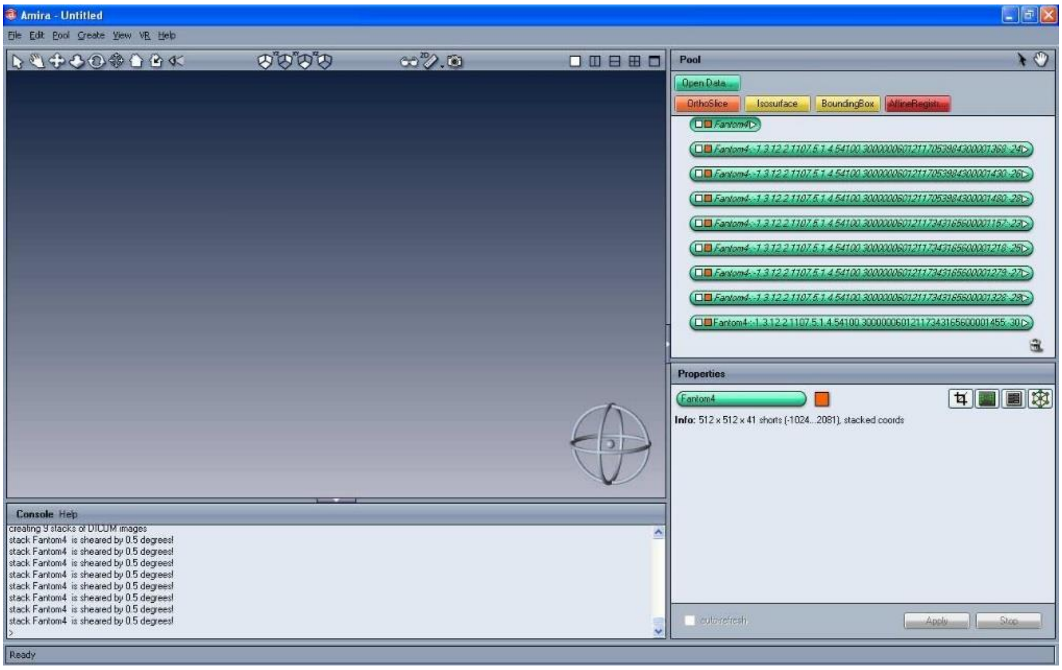

Figure 4. The data is represented as green icons

(source: own study)

4. Data visualization

Object data can be visualized by attaching display modules represented by the color yellow. Clicking on the icon displays a menu from which we can choose several visualization methods, e.g., displaying isosurfaces.

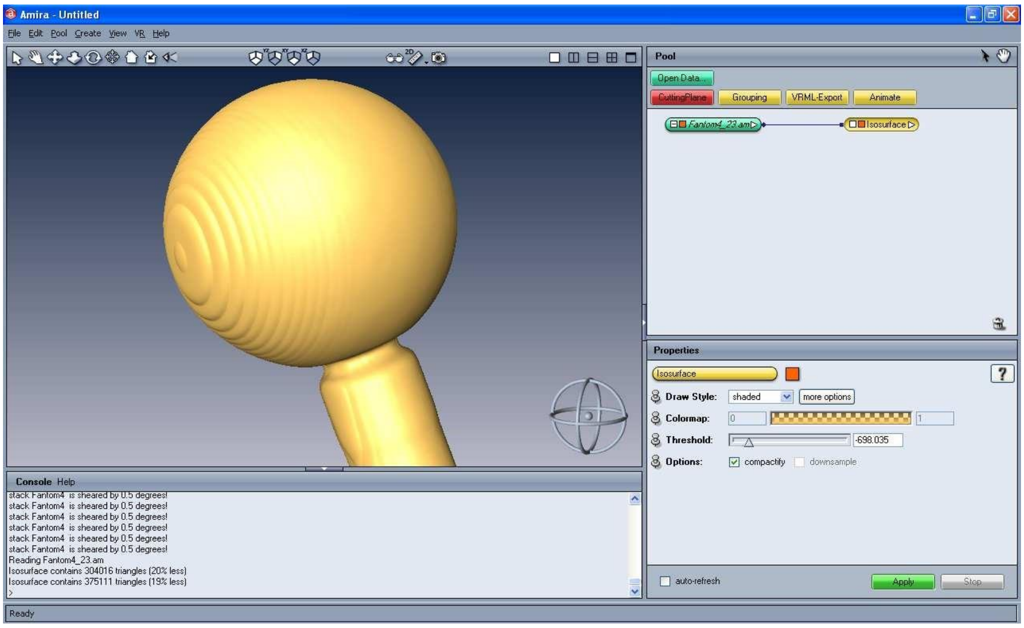

Figure 5. Isosurface generated for a sample Fantom 3 reference sphere

(source: own study)

As can be seen in Figure 5, the generated surface is not perfectly spherical. Methods for smoothing the surface will be presented later, but such actions should always be analyzed.

In the window displaying the surface, we can view the object from every side using, for example, the navigation compass located in the lower right corner of the window.

The first step to fully reflect the object under study is to perform 3D image segmentation. Segmentation assigns each pixel of the image a layer describing which area or material the pixel belongs to. This can be done with the Labelling function and then LabelField or LabelVoxel. The LabelField module allows us to perform manual segmentation using various types of tools, while the LabelVoxel module performs automatic segmentation using information stored in the tomograph data. Figure 6 shows the effect of automatic segmentation.

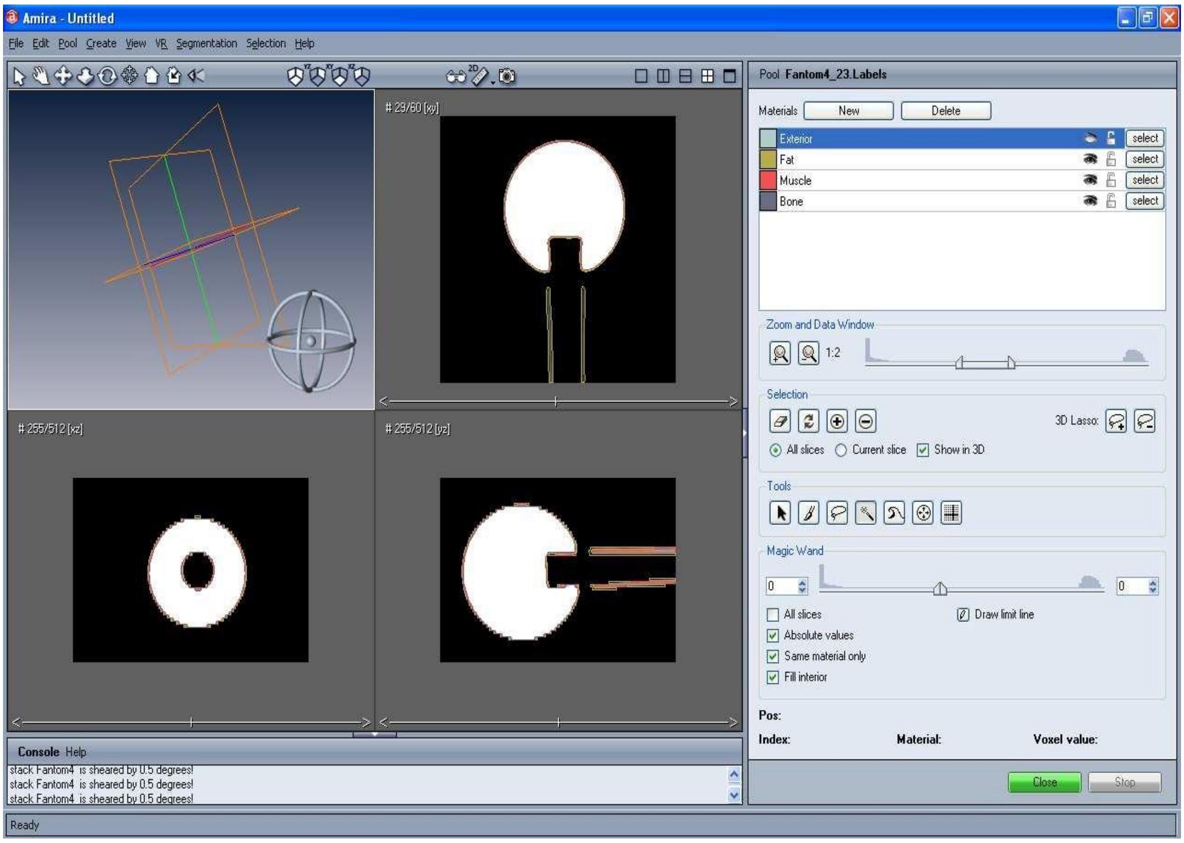

Figure 6. Result of automatic segmentation

(source: own study)

During segmentation, we can clean up the image, e.g., by removing pixels not assigned to layers, known as islands (Remove Island option), and smoothing layers (Figure 6).

It is possible to reduce the so-called staircase effect occurring on the surface of an element. We perform this operation by attaching the InterpolateLabels calculation module to the icon created after segmentation. This module inserts additional "slices" between the base "slices". The program sets the recommended distance between the "slices" and allows you to select the layer for which the interpolation is to be performed (Figure 7).

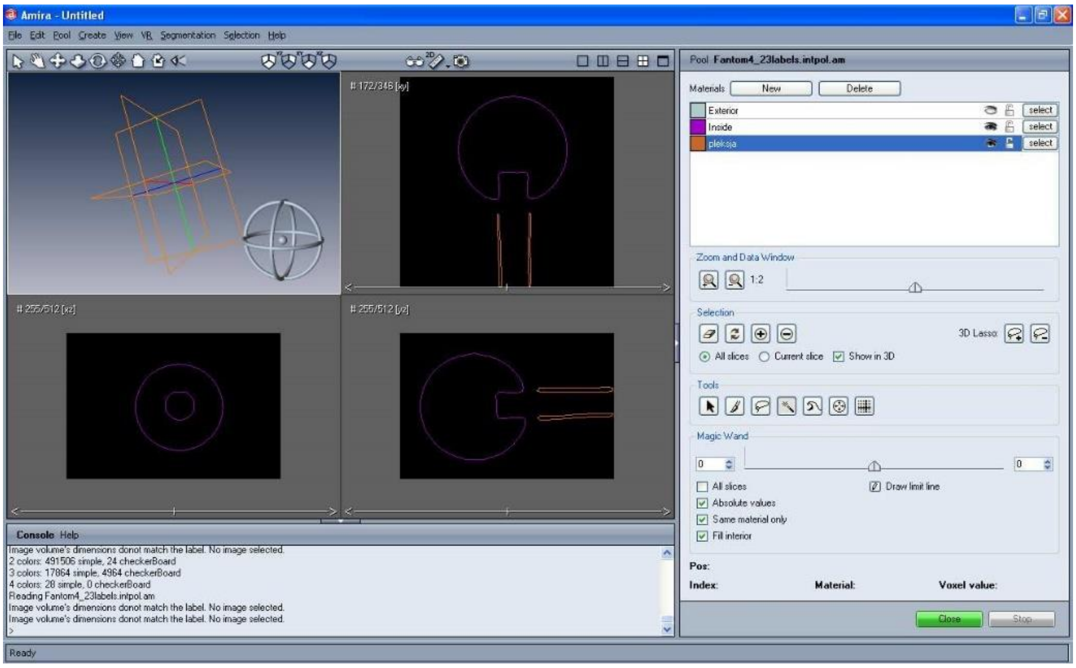

Figure 7. View of layers after interpolation

(source: own study)

The next step is to generate a surface using the SurfaceGen module connected to the icon created after interpolation. After launching, the program performs calculations and creates a surface from the layers created during segmentation. Figure 8 shows the created surface displayed thanks to the connected SurfaceView module.

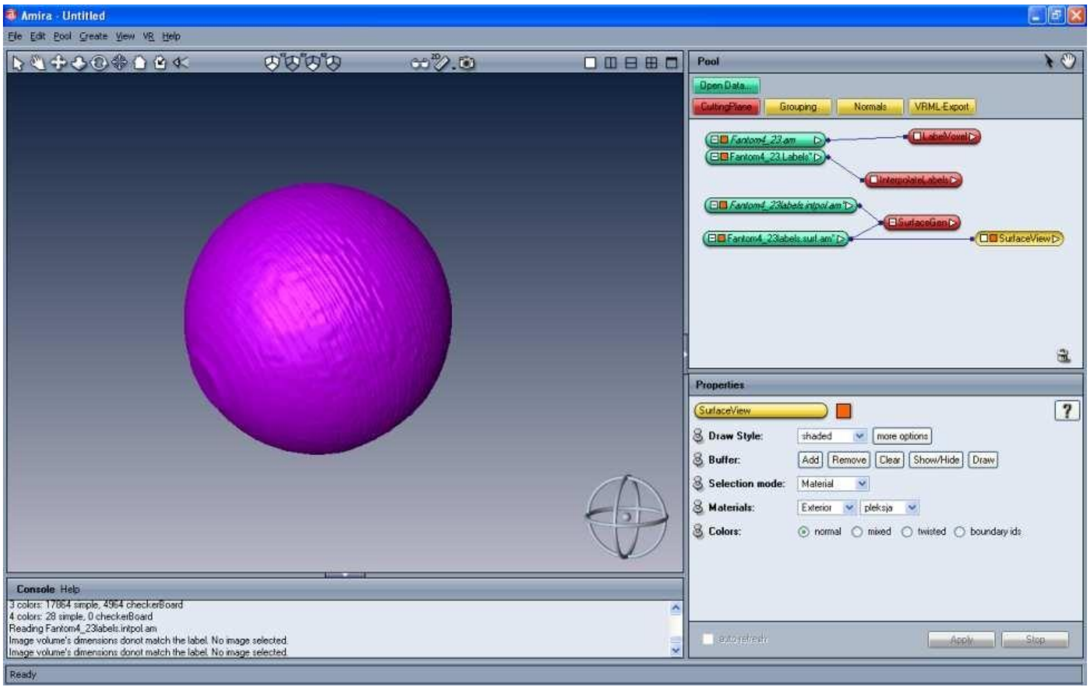

Figure 8. Generated surface after segmentation and interpolation

(source: own study)

In the SurfaceView properties, we can specify what surface is to be displayed and how, e.g., a point cloud or a transparent view.

Figure 8 shows that the surface of the sphere is not yet smooth. To change this, we can use the SmoothSurface module, but first we can simplify the surface, as the created surface may have too many triangles for further operations. The Simplifier editor in the Properties window is used for simplification. After setting the number of triangles, click the Simplify now button and wait for the program to finish simplifying. Figure 9 shows the effect of modifying the surface with a visible triangle mesh.

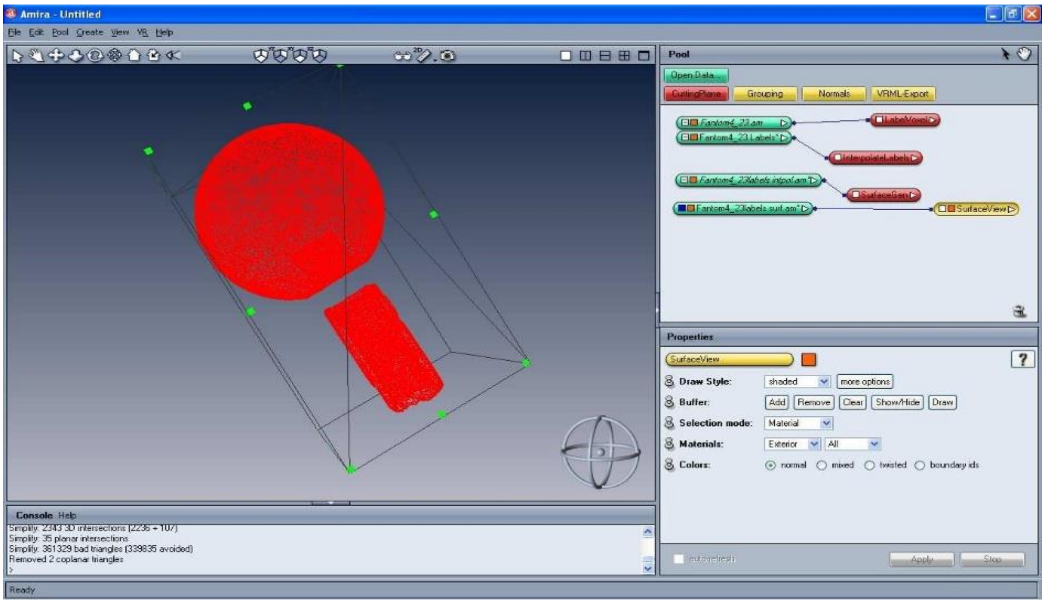

Figure 9. A mesh composed of triangles after simplifying the surface

(source: own study)

After this transformation, we can smooth the surface if necessary. In the SmoothSurface module properties, we set the number of iterations. Figure 10 shows the result of the algorithm.

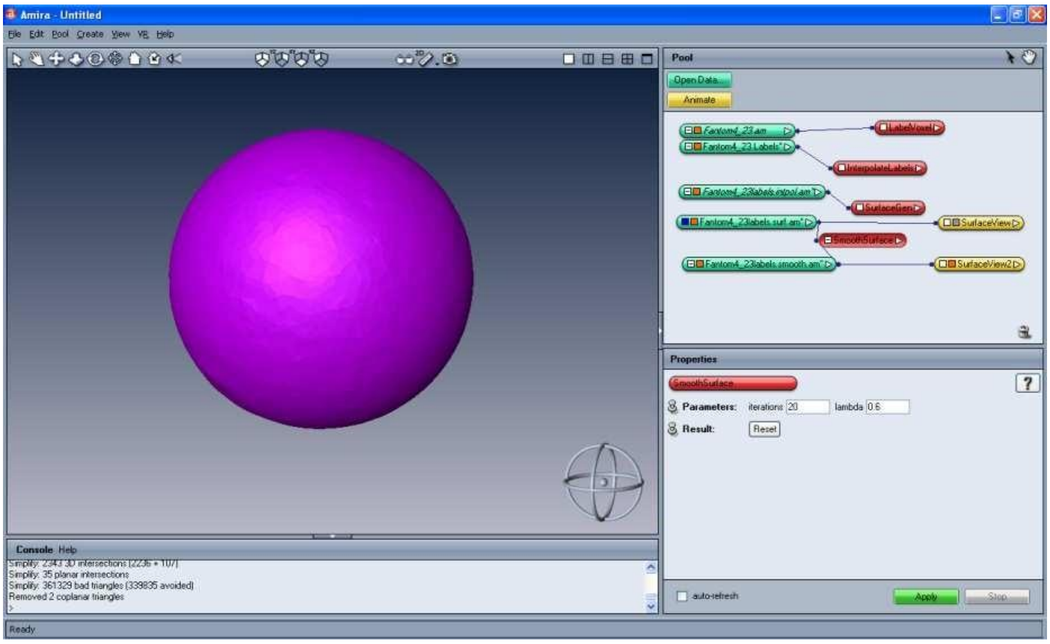

Figure 8. View of the generated surface of the reference sphere after smoothing

(source: own study)

Computer operations that modify the shape of the object under examination introduce specific geometric changes and may also introduce dimensional changes in relation to the actual object. The magnitude of these changes should be analyzed, especially in relation to metrological activities.

5. Generating a tetrahedral mesh

To begin working on creating a tetrahedral mesh, you need a surface composed of triangles. This surface is the result of a previous reconstruction. In this example, it is Fantom3labels.smooth.surf. The surface to be converted into a tetrahedral mesh must meet several requirements, e.g., it must be a closed surface. To check this, we use the Surface Editor located in the properties window. The menu of this editor allows you to perform six tests useful for preparing a tetrahedral mesh. In this work, three tests were used: the Intersection test, the Closedness test, and the Orientation test.

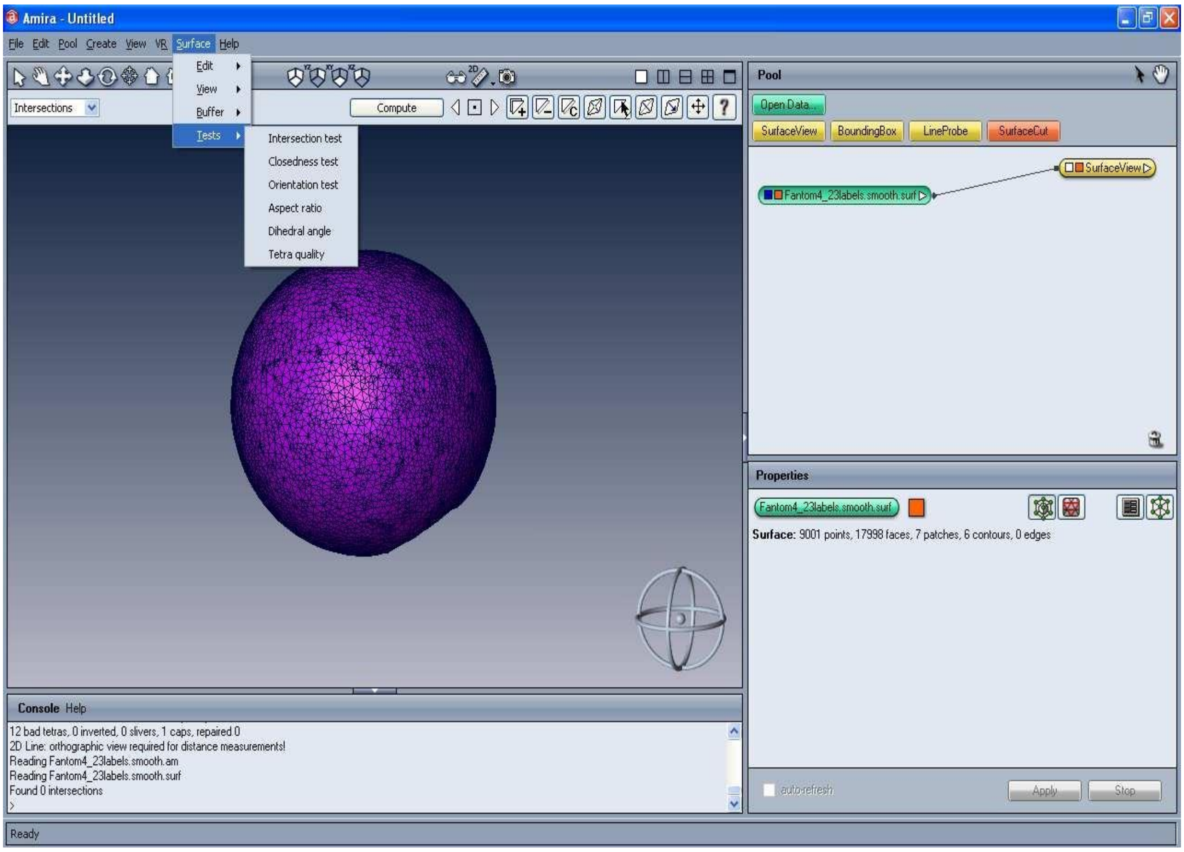

Figure 11. Editing surfaces before generating a tetrahedron mesh

(source: own study)

After successfully passing the verification tests, we proceeded to generate a tetrahedral mesh. We attached the TetraGen module, selected the surface we wanted to convert into a tetrahedral mesh in the properties window, and clicked Run now. After the calculations were completed, a view of a solid composed of a tetrahedral mesh was displayed, which is the basis for creating various views of the internal parts of the object, e.g., cross-sections, and for numerical simulations in finite element analysis (Figure 12).

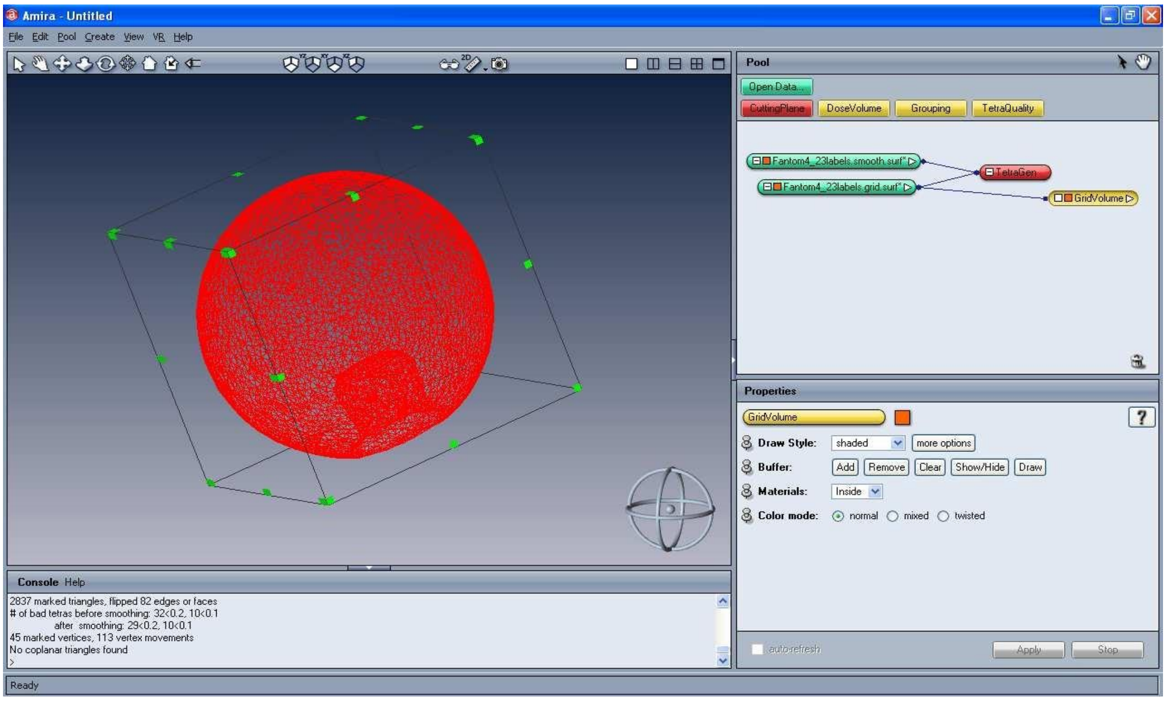

Figure 12. View of a tetrahedral mesh

(source: own study)

6. Measurement of reference balls

The Measuring module available from the View menu was used for the measurements. The diameter and radius of each reference sphere were measured ten times in the XY and YZ planes. The standard deviation was then calculated for each measurement.

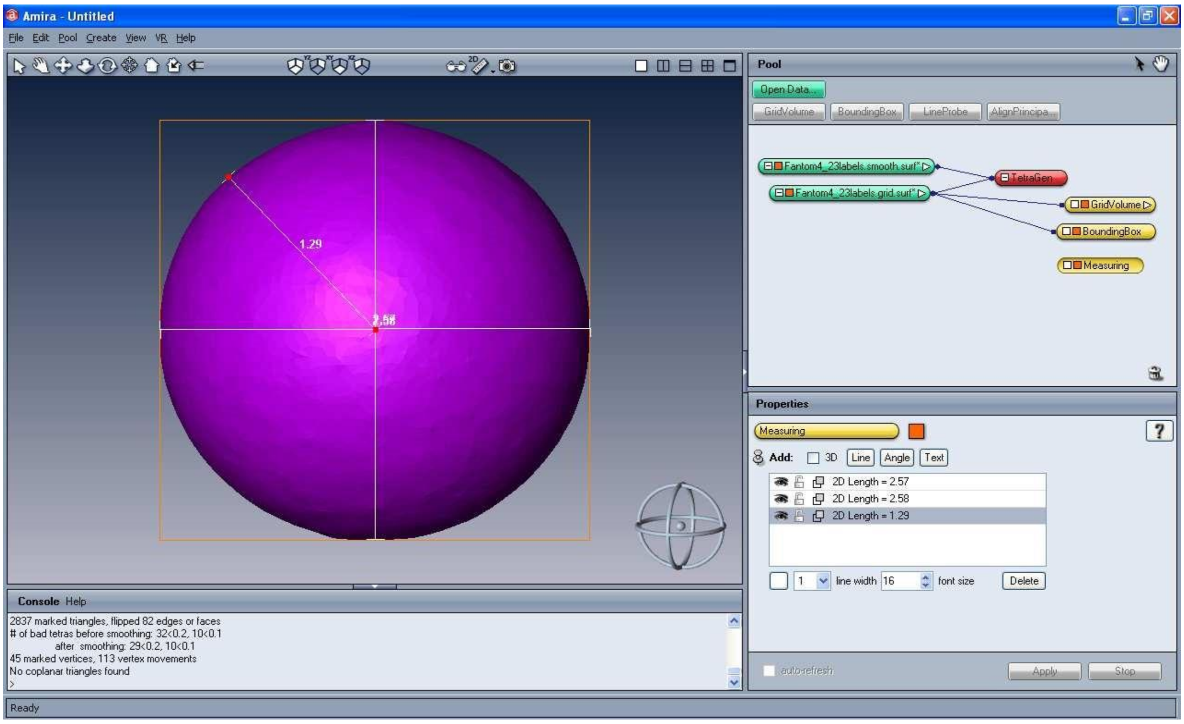

Figure 13. Measurement of a ball marked Fantom 1 with a nominal diameter of Ø = 25.7

(source: own study)

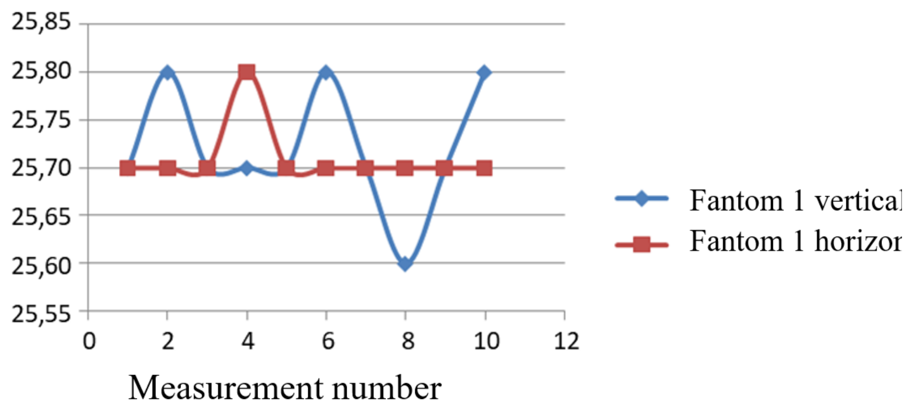

Figure 14. Chart of measurement results Fantom1

(source: own study)

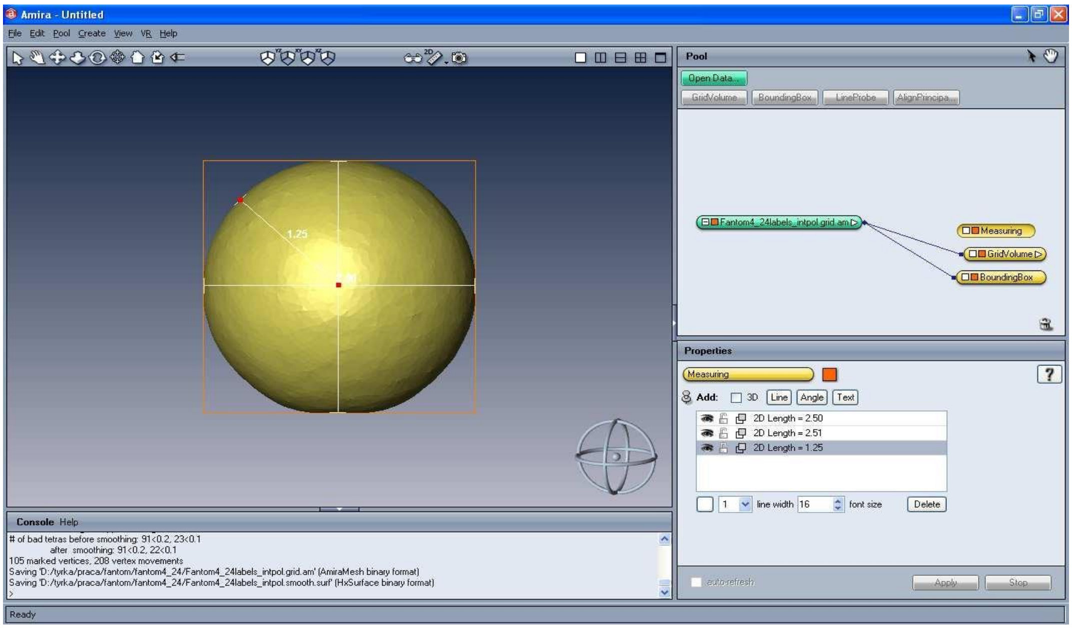

Figure 15. Measurement of a ball marked Fantom 2 with a nominal diameter of Ø = 25.7 [mm]

(source: own study)

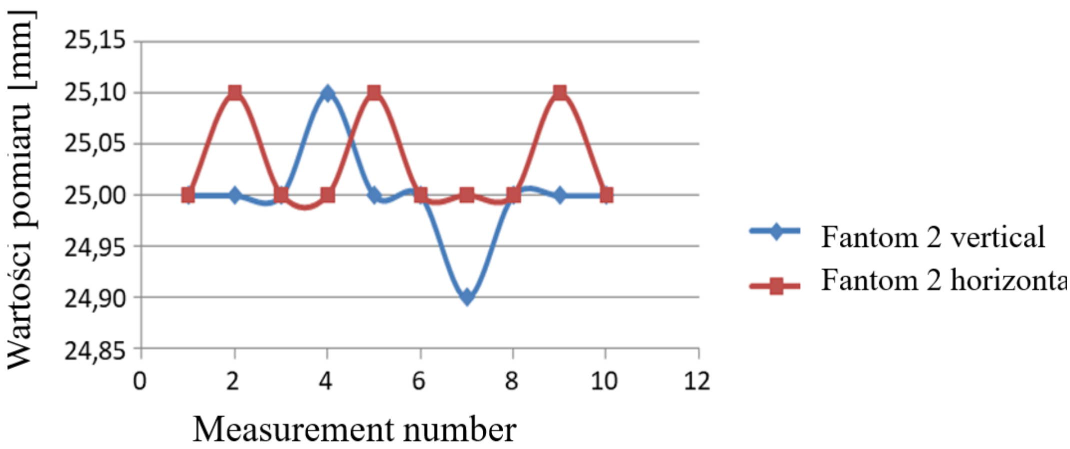

Figure 16. Chart of Fantom2 diameter measurement results

(source: own study)

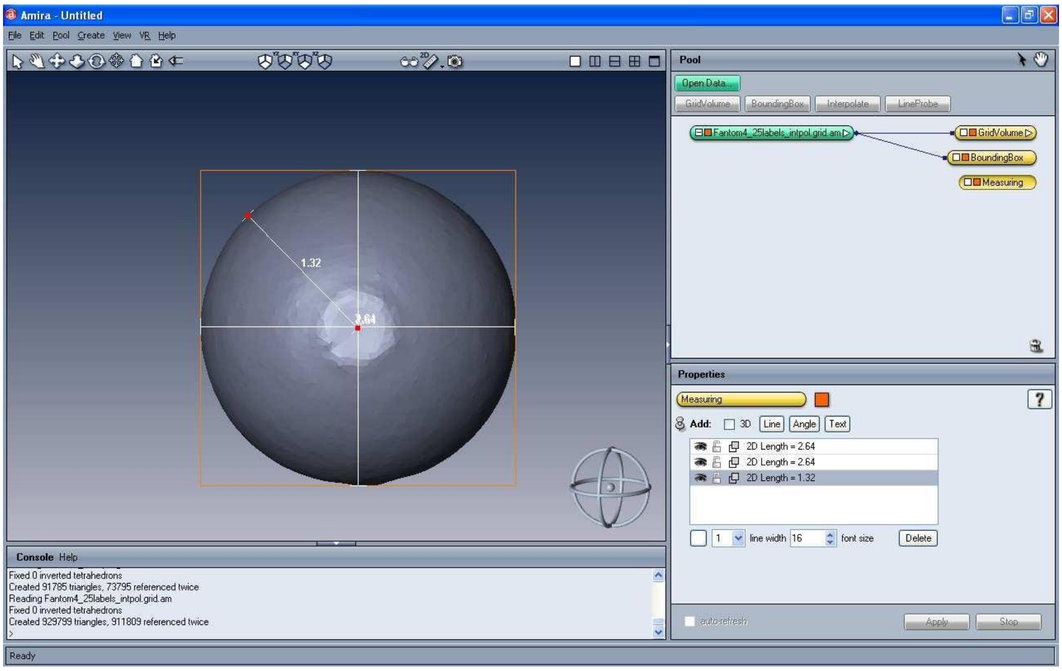

Figure 17. Measurement of a ball marked as Fantom3 with a nominal diameter of Ø = 26.4 [mm]

(source: own study)

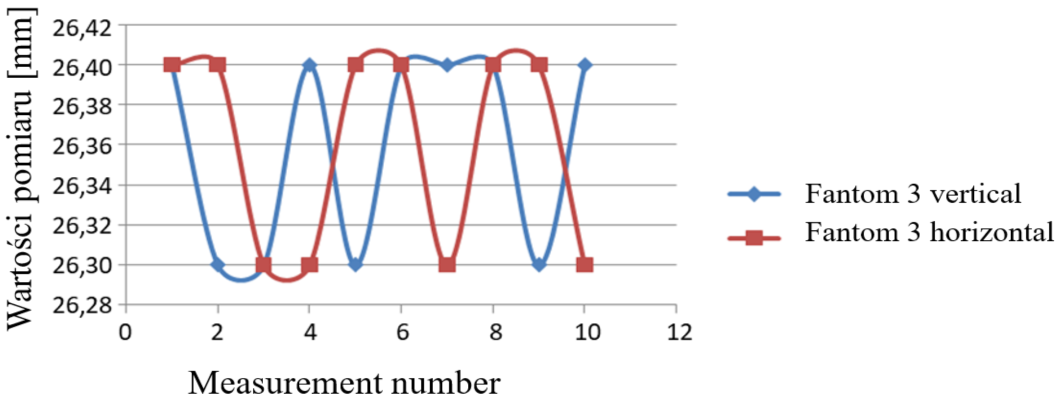

Figure 18. Chart of Fantom3 diameter measurement results

(source: own study)

Analyzing the results obtained, it can be concluded that in computer imaging, an important issue is the correct selection of diagnostic parameters and the positioning of the diagnosed products in the adopted reference system of the computed tomography scanner.

7. Conclusions

In recent years, the use of computed tomography as a control and measurement device has become increasingly popular (Bartscher et al., 2017). The process of three-dimensional visualization can be useful not only in medicine, but also in industry for assessing the quality of products or technological devices (De Chiffre, Carmignato, Kruth, Schmitt, Weckenmann, 2014).

The non-invasive technique of taking measurements using a tomograph is increasingly being used for digital imaging (Thompson et al., 2018).

The use of tomography in industry creates new opportunities for quality control. X-rays allow complex shapes to be examined without the need to dismantle them or create new cross-sections. Devices using X-ray computed tomography allow for the measurement of parts with complex shapes and their internal structure, as well as for the comparison of the obtained metrological results with CAD models.

Modern three-dimensional optical methods have many advantages: they are fast, non-contact, and can be integrated into the production process, e.g., the Metrotom-scatter Control diagnostic system from Zeiss (Kruth et al., 2011).

References

Bartscher, M., Hilpert, U., Goebbels, J., Weidemann, G. (2007). Enhancement and proof of accuracy of industrial computed tomography (CT) measurements. *CIRP Annals – Manufacturing Technology, 56,* 495-498.

Bircher, B., Meli, F., Küng, A., Thalmann, R. (2019). CT geometry determination using individual radiographs of calibrated multi-sphere standards. *e-Journal of Nondestructive Testing, 24*(3). DOI: https://doi.org/10.58286/23677.

Blažek, P., Šrámek, J., Zikmund, T., Kalasová, D., Hortvík, V., Klapetek, P. (2019). *Voxel size and calibration for CT measurements with a small field of view. Proceedings of iCT 2019.*

Busch, M., Hausotte, T. (2024). Practical Approaches for Determining the Structural Resolution Capability of X-ray Computed Tomography Measurement Tasks. *Metrology, 4*(3), 457-468. DOI: https://doi.org/10.3390/metrology4030028.

De Chiffre, L., Carmignato, S., Kruth, J.P., Schmitt, R., Weckenmann, A. (2014). Industrial applications of computed tomography. *CIRP Annals, 63*(2), 655-677.

Ketcham, R.A., Mote, A.S. (2019). Accurate measurement of small features in X-ray CT data volumes, demonstrated using gold grains. *Journal of Geophysical Research: Solid Earth, 124,* 3508-3529. DOI: https://doi.org/10.1029/2018JB017083.

Kruth, J.P., Bartscher, M., Carmignato, S., Schmitt, R., De Chiffre, L., Weckenmann, A. (2011). Computed tomography for dimensional metrology. *CIRP Annals – Manufacturing Technology, 60*(2), 821-842. DOI: https://doi.org/10.1016/j.cirp.2011.05.006.

Liu, W., Chen, X., Zeng, W., Sun, W., Gorman, D., Wilson, A., Qi, Q., Scott, P., Jiang, J., Lou, S. (2024). Comparison of X-ray computed tomography and coordinate-measuring system dimensional measurement for additive manufacturing parts using physical and simulation methods. *Measurement, 229,* 114414. DOI: https://doi.org/10.1016/j.measurement.2024.114414.

Ryniewicz, A. (2009). The analysis of the geometry of osseous tissue of the biological bearings interaction zone in the aspect of accuracy of shape mapping. In: *XIX IMEKO World Congress – Fundamental and Applied Metrology*. Lisbon.

Scherberich, J., Windfelder, A.G., Steinbart, J., Krombach, G.A. (2025). Measurement accuracy of CT systems: The importance of calibration phantoms. *PLoS ONE, 20*(9). DOI: https://doi.org/10.1371/journal.pone.0332263.

Stolfi, A., De Chiffre, L., Carmignato, S. (2016). 3D artefact for concurrent scale calibration in Computed Tomography. *CIRP Annals, 65*(1), 499-502.

Thompson, A., Maskery, I., Leach, R. (2016). X-ray computed tomography for additive manufacturing: A review of metrological challenges. *Measurement Science and Technology, 27*(7), 072001. DOI: https://doi.org/10.1088/0957-0233/27/7/072001.

Zemek, M., Blažek, P., Salplachta, J., Zikmund, T. et al. (2025). Scale Correction in Submicron Computed Tomography with a Submillimeter Field of View. *Tomography of Materials and Structures, 7,* 100054. DOI: https://doi.org/10.1016/j.tmater.2025.100054.